



## The Rheology Behavior of Aramid and Cellulose Nanowhisker Suspensions

Amir Kaveh , Omid Moini Jazani\* , Morteza Ahmadi Lashaki , Mehrzad Mortezaee , Mahmoud Razavizadeh

1. Department of Chemical Engineering, Faculty of Engineering, University of Isfahan, Isfahan, Iran. E-mail: p90132910@aut.ac.ir
2. Department of Chemical Engineering, Faculty of Engineering, University of Isfahan, Isfahan, Iran. E-mail: o.moini@eng.ui.ac.ir
3. Department of Chemical Engineering, Iran University of Science & Technology, Tehran, Iran. E-mail: ahmadi.morteza@yahoo.com
4. Faculty of Materials and Manufacturing Engineering, Malek Ashtar University of Technology, Tehran, Iran. E-mail: mortezaee@mut.ac.ir
5. Faculty of Materials and Manufacturing Engineering, Malek Ashtar University of Technology, Tehran, Iran. E-mail: razavi\_75@yahoo.com

ARTICLE INFO	ABSTRACT
<p><b>Article History:</b> Received: 10 October 2021 Revised: 27 November 2021 Accepted: 28 November 2021</p> <p><b>Article type:</b> Research</p> <p><b>Keywords:</b> Aramid, Cellulose Nanocrystal CNC, Flow Response, Nematic Behavior, Rheology</p>	<p>The flow responses of aramid and cellulose nanowhisker (fibrils) or CNCs (cellulose nanocrystal) suspended in a sulfuric acid and water respect at loadings of about 17% weight fraction was determined in transient shear flow. The effect of temperature and shearing conditions were examined. Aramid solution exhibits strong shear thinning with power-law indices of about 0.2-0.3, and cellulose nanowhisker suspension indices is below 0.15. Formation of an interacting flocculated network at rest is the reason for the large relative viscosity and offers the least flow resistance during shear flow. The structure formed at rest is easily destroyed, and this is the reason for the observed shear thinning. Evolution of shear stress data versus time over four of shear rate were described the structure of nematic phase in aramid/sulfuric acid solution. Also, nanowhisker/water suspension shear rheology results show shear thinning behavior, and behave as a plastic system at different temperatures. For the spinning process, the aramid/sulfuric acid dope through the air gap entered cold water. Orientation of polymer solution emerged from the spinneret and, through very high extensional shear in the air gap, resulted in excellent tensile properties of the final spun fibers.</p>

## Introduction

Liquid-crystalline materials have a wide range of uses, which has spawned new fields of academic and industry study. Some current materials are spun into high-strength fibers from their liquid crystalline form. A liquid-crystalline (LC) solution is a directionally organized liquid with the fluidic characteristics of a liquid. Nematic, smectic, and cholesteric LC phases are characterized according to their degree of order and molecular alignment [1]. Nematic liquid crystals are made up of a series of parallel elongated molecules that are movable in three

\* Corresponding Author: O. M. Jazani (E-mail address: o.moini@eng.ui.ac.ir)



dimensions and can spin owing to the lack of a periodic arrangement. However, because the average distance between molecules is lower than their diameter, rotation is not free, and considerable intermolecular interactions occur. Although nematic liquid crystals have fluid-like qualities and are less dense than smectic liquid crystals, this may result in complicated flow behaviors. In reality, nematic liquid crystals have the lowest structural order among thermotropic liquid crystals, and when heated, they change to an isotropic liquid without passing through another mesophase transition. From a visual standpoint, they are uniaxial, with the optic axis parallel to the mean direction of the long molecule axes, known as the nematic director. Poly(p-phenyleneterephthalamide) (PPTA), a rigid-rod polymer, has a high tensile strength, exceptional stiffness, and great thermal stability [2]. One of the most fascinating physical properties of PPTA macromolecules is their capacity to self-organize and form LC phases in a suitable solvent, such as pure sulfuric acid (H<sub>2</sub>SO<sub>4</sub>) [3]. The strong molecular arrangement is due to the extreme anisotropy of stiff PPTA and the breakdown of intermolecular hydrogen bonds in PPTA caused by the super-acidity of H<sub>2</sub>SO<sub>4</sub>. When heated to 80–95 °C, a nematic sulfuric acid LC solution of PPTA, referred to as PPTA-H<sub>2</sub>SO<sub>4</sub>, with a weight concentration range of 15–20 percent, was used to manufacture high-strength fibers utilizing the dry-jet wet-spinning process [4–6]. Strong shear-thinning, lengthy relaxation time, and high viscous activation energy have been described as peculiar rheology features of PPTA-H<sub>2</sub>SO<sub>4</sub> LC solution [7–11]. In the optically isotropic zone, the viscosity of the solution increases with concentration and reaches a maximum. The solution becomes optically anisotropic (liquid crystalline) at concentrations above this maximum, and its viscosity drops to a minimum before increasing again. We decided to look into the rheological features of the PPTA-H<sub>2</sub>SO<sub>4</sub> LC solution system in the spinning process because of this unusual behavior. Many studies on the preparation of cellulose nanoparticles have lately been conducted [12]. Nanocrystalline cellulose (NCC) is a rigid rod of cellulose that is also known as cellulose whisker (CW) and cellulose nanocrystal (CNC). In aqueous suspensions, these rod architectures display complicated colloidal phase and rheological behaviors, with their characteristics influenced by volume fraction and inter-particle forces [15]. The behavior of re-entrants the conflicting effects of double layer thickness and interparticle twisting may be described for nanocrystalline cellulose suspensions [13]. The effects of various acids on the rheology and aggregation behavior of 2,2,6,6-tetramethylpiperidine-1-oxyl radical (TEMPO) cellulose nanofibrils were investigated by Alves et al. [14]. They discovered that phosphate ions caused substantial aggregation at pH 2.3, resulting in big particles and highly strong gels [12]. To make the PBST/CNC composites, Wang et al. [16] produced polybutylene succinate-co-terephthalate (PBST) copolymers with varied BS/BT unit ratios and blended them with cellulose nanocrystals (CNC) by melt blending. Their findings revealed that the CNC is well dispersed in the PBST matrix, forming a network-like structure, and that the PBST composite has a robust reinforcing effect.

The water suspensions often display severe shear thinning in addition to the fibril level features of nanowhisker. The cause of the extreme shear thinning that has been noticed is yet unknown. The isotropic-nematic phase ordering was predicted to dominate the shear viscosity behavior in nanowhiskers, which have more homogenous particle shapes and sizes [18]. However, some aspects of the experimental data contradict the conclusions: The standard S-shaped flow curves for such a procedure were not seen, and a necessity to disrupt the flocculation was recorded during sample processing. The observed power-law flow curves are more typical for slightly attracting colloids, which is consistent with prior CNF results [19]. The rheology of cellulose nanowhisker/water suspensions under transient shear rates at different temperatures is investigated in this paper. Our findings in this research give some basic understanding of the LC spinning process.

## Experimental

### Materials

Sulfuric acid containing 0.2 wt% surplus SO<sub>3</sub> was made by combining fuming sulfuric acid (25 wt%) with concentrated sulfuric acid (98 wt percent). Acid-base titration was used to determine the concentration of sulfuric acid.

### Polymerization Process

P-aramid is synthesized in solution from the monomers 1,4-phenylene diamine (Merck chemical company, Germany) and terephthaloyl chloride (Merck chemical company, Germany) in a condensation reaction yielding hydrochloric acid as a byproduct. To the production of P-aramid polymer, the dried calcium chloride (CaCl<sub>2</sub>, Merck chemical company, Germany, 10mol) and the purified tributyl amine (TNBA, Merck chemical company, Germany, 23mol) was dissolved in purified N-methyl-2-pyrrolidone (NMP, Merck chemical company, Germany, 30lit). The polymerization reaction was carried out in a batch mixer (70lit). The mixing temperature in the first stage was 60<sup>0</sup>C (the blade rotation speed was 100rpm). The process was carried out under an N<sub>2</sub> atmosphere. After 10 min, the mixture temp was adjusted to 25<sup>0</sup>C, and the first monomer, 1,4-phenylene diamine (PPD,14mol) was added to the mixture, and its temp was decreased to zero. The dried second monomer, terephthaloyl chloride (TCL,14mol) was added to mix slowly; in this stage of the reaction the mixture temperature was adjusted to about 5<sup>0</sup>C. The mixing process continued for 30 min (time of polymerization reaction); after this time, the color of the mixture was milky when the mixing process was stopped, its color was amazing.

### Inherent Viscosity

The formula for calculating inherent viscosity (I.V.) is  $I.V.=\ln(\text{rel}/c)$ , where  $c$  is the concentration (0.5 gram of polymer in 100 ml of concentrated sulfuric acid) and  $\text{rel}$  is the ratio between the flow times of the polymer solution and the acid as measured at 300 degrees Celsius. Cannon capillary Ubbelohde viscometer was used for the calculation of inherent viscometry.

### Preparation of PPTA and H<sub>2</sub>SO<sub>4</sub> dope and Fibre Spinning

The spinning apparatus contains a mixer (5lit) for mixing PPTA and H<sub>2</sub>SO<sub>4</sub> in several steps. Temperature sets at 82<sup>0</sup>C. The mixture was mixed for 80 min. PPTA/H<sub>2</sub>SO<sub>4</sub> dope guided to the extruder for homogenizes dope mixture. The solution was extruded at a constant rate through a stainless-steel spinneret. After extrusion, the fiber passed an air gap of 10 cm and entered a water bath of 4<sup>0</sup>C. Finally, the filaments were collected on a wind-up wheel. The fiber samples were washed with NaOH solution to neutralized acid then washed with water for several days to remove remaining solvent and then dried under vacuum at 80<sup>0</sup>C for 2 days.

### Preparation of H<sub>2</sub>SO<sub>4</sub>-Hydrolyzed CNCs

This approach was used to create H<sub>2</sub>SO<sub>4</sub>-hydrolyzed CNCs. Cotton linter bits were milled after being chopped into little pieces. Sulfuric acid (100mL, 64 wt%) was added to 10 gr of milled Cotton in a 500 mL round-bottom flask warmed to 450<sup>0</sup>C. The reaction was carried out at 450<sup>0</sup>C for 45 minutes with mechanical stirring before being stopped by diluting the reaction liquid with 300 mL of cold DI water. Repeated centrifugation at 250C and 4500 rpm for 15 minutes eliminated the acid from the CNC suspension. The sediment was collected after the fifth centrifugation.

## Rheological Measurements

Subsequently, the PPTA-H<sub>2</sub>SO<sub>4</sub> and CNC/H<sub>2</sub>O dope solutions were performed with a rotational rheometer (RC20 Rheotec Instruments, CC14 Measuring System) at three temperatures (75, 80, 85°C) for PPTA-H<sub>2</sub>SO<sub>4</sub> dope and four temperatures (10, 20, 30, 40°C) for CNC/H<sub>2</sub>O dope in the shear rate range of 10–1032 s<sup>-1</sup>.

## Results and Discussion

Temperature effect on shear viscosity ( $\eta$ ) as opposed to shearing condition ( $\dot{\gamma}$ ) of PPTA/H<sub>2</sub>SO<sub>4</sub> dope is shown in Fig. 1.

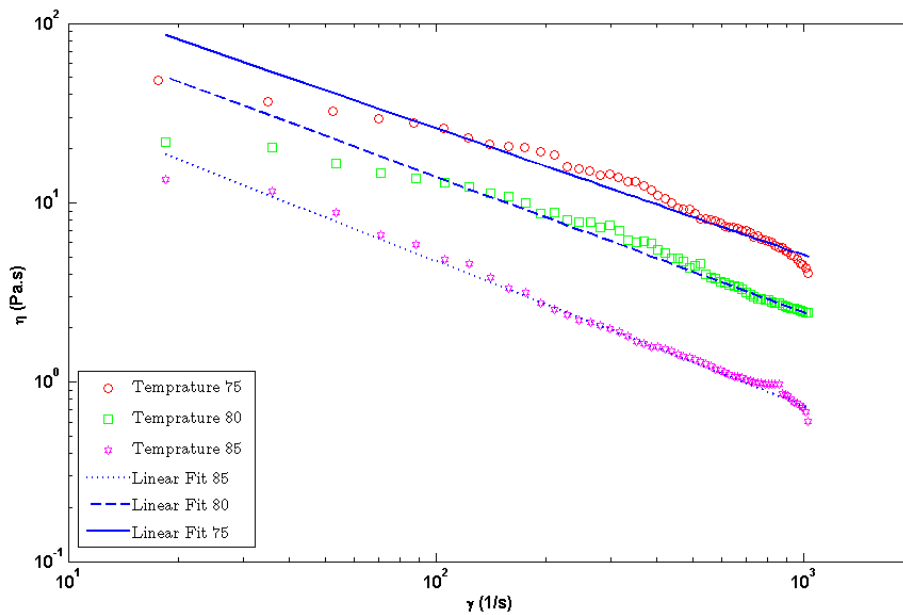


**Fig. 1.** Temperature dependence of shear viscosity ( $\eta$ ) of PPTA/H<sub>2</sub>SO<sub>4</sub>, dope as a function of shearing condition ( $\dot{\gamma}$ )

Throughout the spectrum, all three PPTA samples show clear shear-thinning behavior. As decreases in direct proportion to. Table 1 shows the slope of a descending line on a logarithmic plot at three temperatures using the power-law equation  $\eta = K \dot{\gamma}^{n-1}$ . Entanglements between macromolecular chains are considered to cause this shear-thinning effect. Shearing rigid-rod polymers like PPTA reduce the number of entanglements, allowing macromolecules to change their structures more quickly. As the temperature rises from 75 to 85 degrees Celsius, the amount of PPTA/H<sub>2</sub>SO<sub>4</sub> dope drops. This type of behavior is common in ordinary polymers. [2] The shear viscosity at 75°C is more than that of the sample at 80 and 85°C since a low temperature is more conducive for aggregation between micelles and can form a dense layered structure, increasing then the shear viscosity.

As can be seen, an increase in temperature leads to a higher power index.

**Table 1.** Power law index of PPTA/H<sub>2</sub>SO<sub>4</sub>, dope in four temperatures

Temperature (°C)	n-1	n	Log(k)
75	-0.80	0.20	5.2483
80	-0.77	0.23	6.3767
85	-0.76	0.24	6.8927

The evolution of shear stress under different shear rates is reported in Fig 2. An increase of shear rate leads to higher shear stress, which related to the higher orientation of nematic phase in LC system and lower relaxation time of stress induced by shear. In addition, the fluctuation of stress increased at higher shear rates. The rise of stress is related to the orientation of the nematic phase with higher domain and network formation along the flow and its fall is associated with the break down of the network. The formation and breakdown of the network are faster at a higher shear rate.

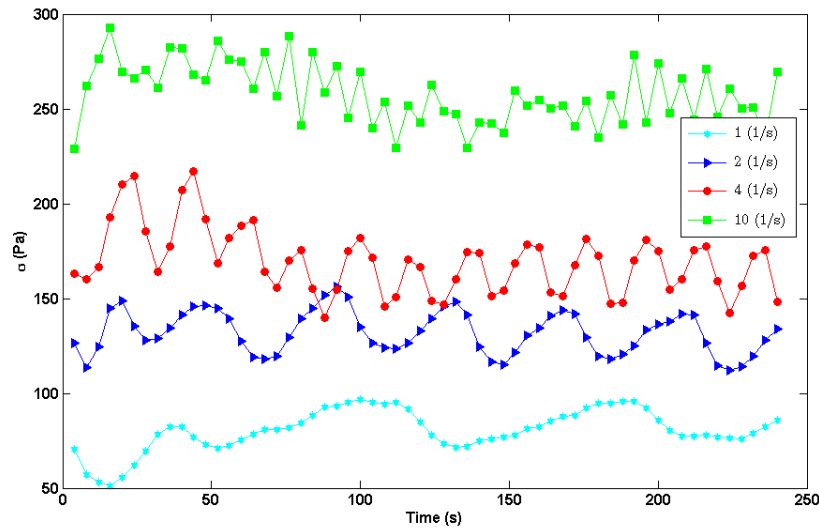


Fig. 2. Shear stress ( $\tau$ ) during 240 sec at different shear strain: PPTA/H<sub>2</sub>SO<sub>4</sub> solution

The evolution of shear viscosity under different shear stresses is reported in Fig. 3. As can be seen, the higher stress leads to faster shear viscosity reduction; by increasing stress, the nematic phase aligns rapidly. Therefore, it is quickly reached to yield stress, and viscosity decreases at higher stress.

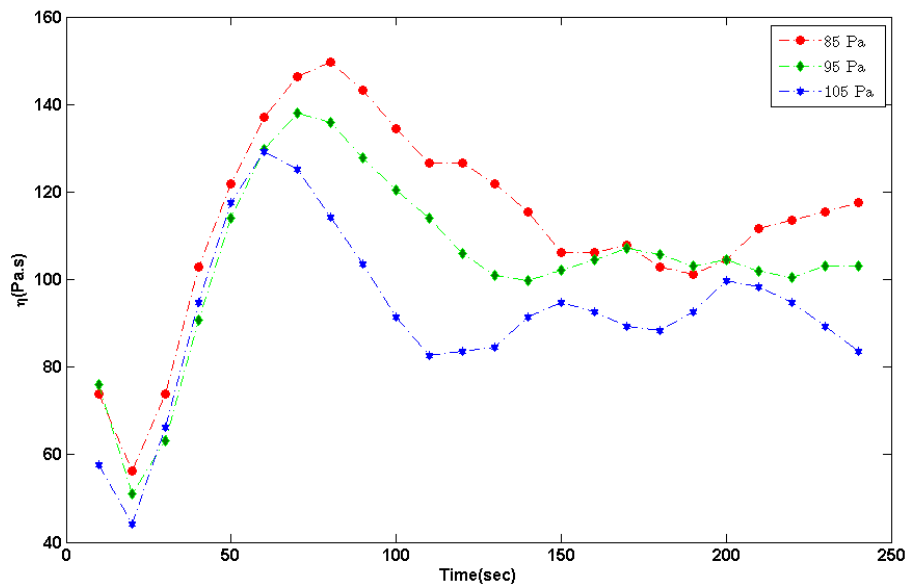
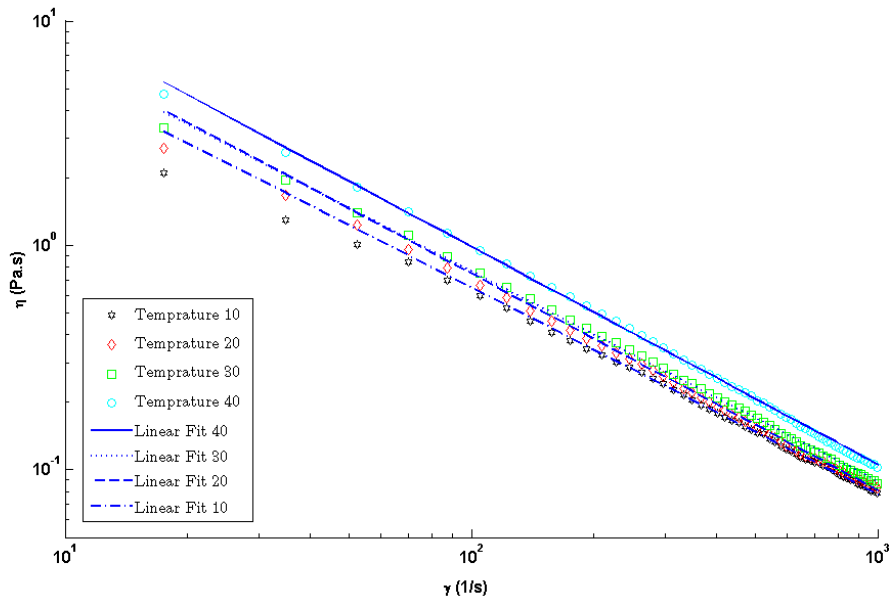


Fig. 3. Shear viscosity ( $\eta$ ) during 240 sec at different shear stress for PPTA/H<sub>2</sub>SO<sub>4</sub> solution



**Fig. 4.** Temperature dependence of shear viscosity ( $\eta$ ) of Cellulose Nanowhisker/H<sub>2</sub>O as a function of shearing condition ( $\dot{\gamma}$ )

Throughout the range, all four Nanowhiskerwater suspension samples demonstrate shear-thinning behavior. As it grows, it lowers in direct proportion to. Table 2 shows the slope of such a falling line on the logarithmic plot. Entanglements between macromolecular chains are considered to cause this shear-thinning effect. As the temperature climbed from 10 to 40°C, the Nanowhisker water suspension increased. An increase in viscosity with increasing temperature can be attributed to changes in microstructure. The cause of temperature-induced viscosity rise in high-concentration samples is unknown, and further research is needed in the future. At higher temperatures, however, Pan et al. found densely packed chiral nematic domains with smaller pitch sizes. [18] may be considered a possible reason which has higher elasticity. Since the high elastic system have lower Power law index, increase of temperature leads to the lower power law index.

**Table 2.** Power law index of Nanowhisker\water suspension in four temperatures

Temperature (°C)	n-1	n	Log (k)
10	-0.85	0.15	3.4042
20	-0.90	0.10	3.7929
30	-0.93	0.07	4.0528
40	-0.96	0.04	4.4645

The evolution of shear stress at two shear rates for four temperatures is reported in Fig. 5. Increase of shear rate leads to the higher shear stress, which is related to the higher orientation of the nematic phase in LC system and lower relaxation time of stress induced by shear. In addition, the fluctuation of stress increased at higher shear rates. The rise of stress is related to the orientation of the nematic phase with higher domain and network formation along the flow, and its fall is related to breakdown of the network. The formation and breakdown of the network are faster at a higher shear rate.

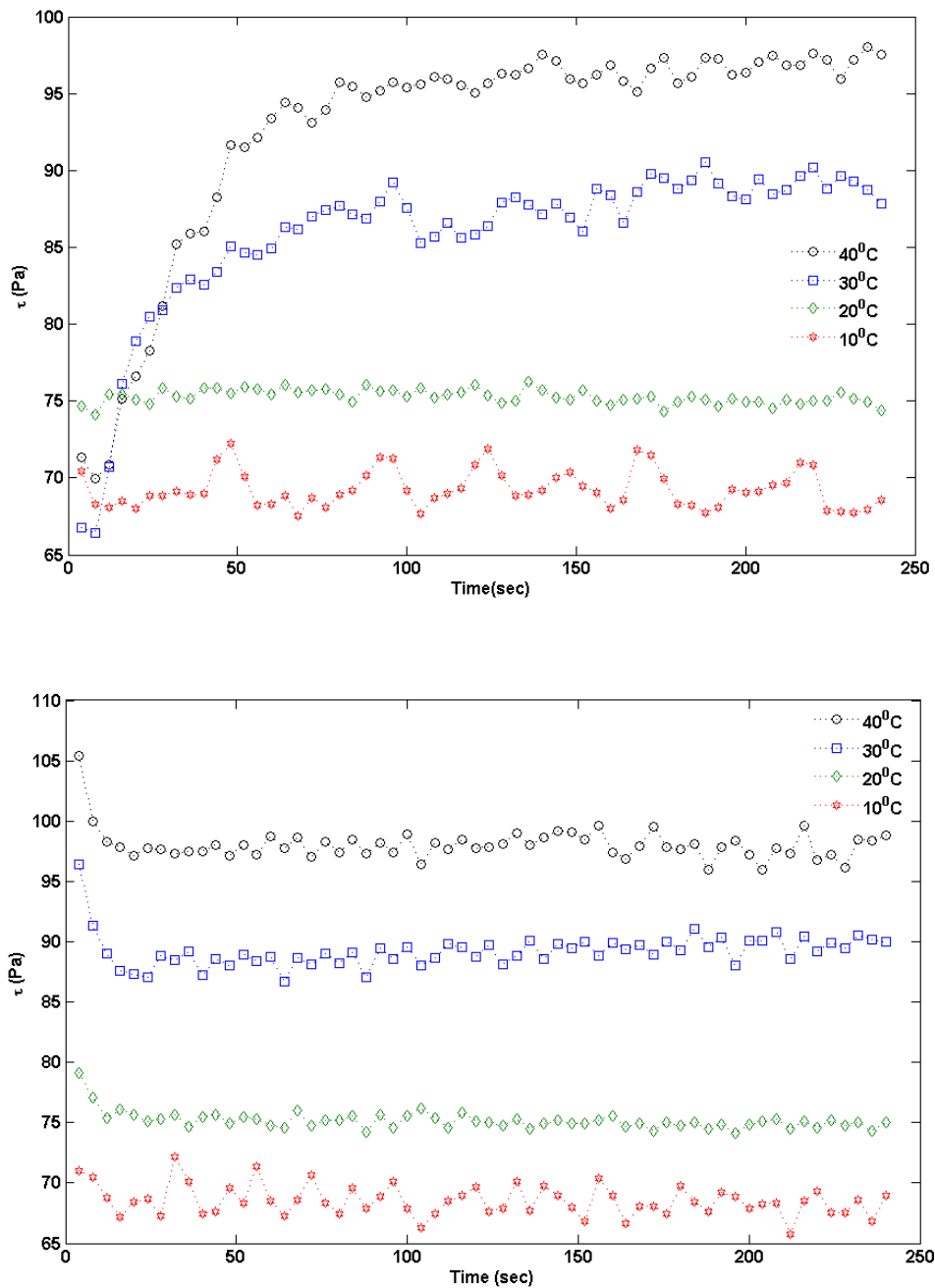


**Fig. 5.** The transient shear response of Cellulose Nanowhisker/H<sub>2</sub>O at shear rate ( $\dot{\gamma}$ ) a) 5 b) 10 (1/s) for different Temperatures

Fig. 5 shows the evolution of shear stress at four temperatures for 5 and 10 1/s shear rates. As can be seen in both shear rates by an increase in temperature, shear stress increased. These are related to microstructural rearrangement of the nematic phase. Another point which can be understood from Fig. 5 is the change of stress at each temperature which increases by reduction of temperature. These are related to the stiffer structure at low temperature, which is destroyed and built up under flow. For a shear rate of 10 sec<sup>-1</sup>, observed yield stress at 5 sec<sup>-1</sup>, with increasing the stress value, the curve gradually reached to plateau state. These indicate that at the higher shear rate, the chance of rearrangement and relaxation of induced stress decreased and, therefore, sample yielded against stress (Table 3).



**Table 3.** Yield stress for different temperature at  $\dot{\gamma} = 10$  (1/sec)

Temperature (°C)	$\tau_y$
10	71
20	78
30	96
40	106

## Conclusion

The rheological properties of liquid crystals were investigated with shear stress. The present study demonstrates that liquid crystals exhibit appreciably different rheological properties. The shear viscosities of the PPTA/sulfuric acid solution show a typical shear-thinning behavior, which obeys the power-law behavior with the power indices of about 0.2. As the temperature increased, the viscosities decreased. The nematic-isotropic transition, in which rod-like molecules lose part of their orientation ordering and become partially isotropic, can explain the temperature dependence of shear viscosity. Rheological results indicate that the studied liquid crystals exhibit fluctuation shear stress during constant shear rate which this fluctuation increased by a higher shear rate. At constant shear stress, firstly, the shear viscosity increased to a maximum, and decreased to a stable value. The increasing viscosity during time is related to preferential alignment along the shear direction and network formation. The decreasing viscosity is related to the yielding of phase alignment and network breakup.

At high concentrations, cellulose nano whisker aqueous solutions display isotropic to chiral nematic liquid crystalline. At this temperature range, when the viscosity increases with increasing temperature, some microstructural change occurs. Increased viscosity, on the other hand, indicates changes in the microstructure or the proportions of isotropic and anisotropic areas.

## References

- [1] Friedel G. Mesomorphic states of matter. *Ann. Phys.* 1922; 18: 273–474.
- [2] Yang H H. *Aromatic High-Strength Fibers*, 1st ed.; Wiley-VCH: New York, NY, USA, 1989; 207–289.
- [3] Zhou M, Frydman V, Frydman L. On the Molecular organization of PPTA in sulfuric acid: an NMR study. *J. Phys. Chem.* 1996; 100: 19280–19288.
- [4] Kiyo V N, Rozhdestvenskaya T A, Serova L D. Rheological properties of liquid-crystalline solutions of poly(p-phenylene terephthalamide) and behavior of the jet in spinning through an air space. *Fibre Chem.* 1997; 29: 81–86.
- [5] Picken S J, Zwaag S V, Northolt M G. Molecular and macroscopic orientational order in aramid solutions: a model to explain the influence of some spinning parameters on the modulus of aramid yarns, *Polymer*, 1992; 33: 2998–3006.
- [6] Slugin I V, Sklyarova G B, Kashirin A I, Tkacheva L V, Komissarov S V. Microfilament yarn for ballistic protection. *J. Fibre Chem.* 2006; 38: 22–24.
- [7] Picken S J, Aerts J, Doppert H L, Reuvers A J, Northolt M G. Structure and rheology of aramid solutions: transient rheological and rheo-optical measurements. *Macromolecules*, 1991; 24: 1366–1375.
- [8] Doppert H L, Picken S J. Rheological properties of aramid solutions: transient flow and rheo-optical measurements. *Mol. Cryst. Liq. Cryst.* 1987; 153: 109–116.
- [9] Picken S J. Phase transitions and rheology of aramid solutions. *Liq. Cryst.* 1989; 5: 1635–1643.
- [10] Picken S J, Aerts J, Visser R, Northolt M G. Structure and rheology of aramid solutions: X-ray scattering measurements. *Macromolecules*, 1990; 23: 3849–3854.
- [11] Baird D G, Ballman R L. Comparison of the rheological properties of concentrated solutions of a rod-like and a flexible chain polyamide. *J. Rheol.* 1979; 23: 505–524.



- [12] Rol F, Belgacem M N, Gandini A, Bras J. Recent advances in surface-modified cellulose nanofibrils. *Prog Polym Sci*, 2019; 88 : 241–264.
- [13] Xu Y, Atrens A, Stokes J R. Structure and rheology of liquid crystal hydroglass formed in aqueous nanocrystalline cellulose suspensions. *Journal of colloid and interface science*, 2019; 555 : 702-713.
- [14] Alves L, Ferraz E, Lourenço A F, Ferreira P J. Tuning rheology and aggregation behaviour of TEMPO-oxidised cellulose nanofibrils aqueous suspensions by addition of different acids. *Carbohydrate Polymers*, 2020; 237: 116109.
- [15] Xu Y, Atrens A, Stokes J R. A review of nanocrystalline cellulose suspensions: Rheology, liquid crystal ordering and colloidal phase behavior. *Advances in Colloid and Interface Science*, 2019; 30361-6.
- [16] Wang J M, Ding S J, Wu T M. Rheology, crystallization behavior, and mechanical properties of poly (butylene succinate-co-terephthalate)/cellulose nanocrystal composites, *Polymer Testing*, 2020; 87: 106551.
- [17] Shojaeiarani J, Bajwa D S, Stark N M., Bajwa S G. Rheological properties of cellulose nanocrystals engineered polylactic acid nanocomposites. *Compos. B Eng*, 2019; 161: 483–489.
- [18] Pan J, Hamad W Y, Straus S K. Parameters Affecting the Chiral Nematic Phase of Nanocrystalline Cellulose Films. *Macromolecules*, 2010; 43: 3851–3858.
- [19] Pääkkö M, Ankerfors M, Kosonen H, Nykänen A, Ahola S, Österberg M, Ruokolainen J, Laine J, Larsson P, Ikkala O, Lindström T. Enzymatic hydrolysis combined with mechanical shearing and highpressure homogenization for nanoscale cellulose fibrils and strong gels. *Bio Macromol*, 2007; 8: 1934-1945.

**How to cite:** Kaveh A, Moini-Jazani O, Ahmadi-Lashaki M, Mortezaee M, Razavizadeh M. The Rheology Behavior of Aramid and Cellulose Nanowhisker Suspensions. *Journal of Chemical and Petroleum Engineering*. 2022; 56(2): 193-201.